Heath, C., Bond, I., & Potter, K. (2016). Interlocking Electro-Bonded Laminates. Journal of Intelligent Material Systems and Structures. DOI: 10.1177/1045389X16672733

Peer reviewed version

Interlocking Electro-Bonded Laminates

C J C Heath, I P Bond and K D Potter

Advanced Composites Centre for Innovation and Science, Department of Aerospace Engineering, University of Bristol, Bristol, BS8 1TR, UK

Email: c.heath@bristol.ac.uk

This paper is a development of the work presented at SPIE Smart Structures Conference 2016 (Heath et al., 2016b)

Abstract

Novel, structurally integrated, interlocking electrode elements are presented in this paper. Electro-Bonded Laminates (EBL) are structures that utilise the electrostatic force of attraction, generated between closely spaced electrode elements when subject to high potential difference (~2 kV), to control internal structural coupling. Control of internal connectivity allows for flexural stiffness modulation, with significant potential applications including vibration suppression and morphing applications. Existing EBL devices use parallel planar electrode elements. For this study Polyurethane (PU) core structures were cast with interlocking geometries based on a simple cosine wave form. By introducing this additional complexity to the electrodes, additional electrode-electrode contact area is available within a set external geometric profile, whilst also introducing directional resistance to sliding motion between the two surfaces. Interlocking Electro-Bonded Laminate (iEBL) devices are demonstrated with electrostatic holding force capabilities similar to equivalent planar devices, with the added benefit of alignment and sliding restrictions provided by the directional elements. A novel enhancement to the existing EBL technology has thus been demonstrated.

Keywords: Electro-Bonded Laminates, Interlocking, Reversible Adhesion

Introduction

Strong electric fields generated from closely spaced electrode elements can generate significant electrostatic forces of attraction which can be utilised to control the structural coupling of laminated elements (Bergamini et al., 2006; Di Lillo et al., 2013; Heath et al., 2016a; Raither et al., 2014; Tabata et al., 2001). Figure 1 is an example of an EBL device, showing conductive elements attached to a host structure and separated by a thin dielectric layer. On/off voltage control provides 'on demand' reversible adhesion, modulating the coupling of the upper and lower sections, and providing varying levels of shear stress transfer. The Coulombic forces between the adjacent electrodes provide a normal attachment force (Coulomb, 1785) which, in combination with the friction of the electrode faces, provides resistance to shearing forces. The effective shear strength of the reversible adhesive interface is determined in part by the applied voltage, thus EBL represent voltage tuneable smart structures.

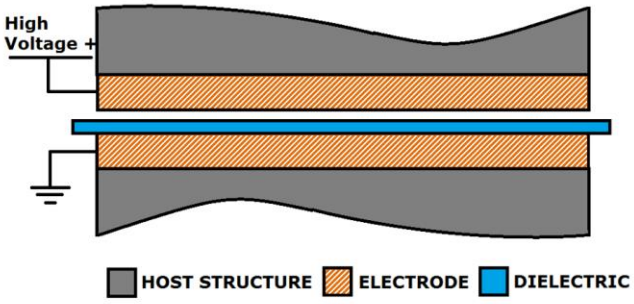

Figure 1: Example of an EBL configuration

The use of high voltage to tailor the structural response of stacked film devices has previously been demonstrated (Tabata et al., 2001). This concept was extended, replacing the permanent adhesive between adjacent layers in a composite beam structure with reversible electrostatic bonding (Bergamini, 2009; Bergamini et al., 2006, 2007). The potential applications for EBL devices are numerous, including morphing structure applications (Previtali et al., 2015; Raither et al., 2012, 2013, 2014), vibration suppression (Bergamini et al., 2006, 2007), or variable stiffness functionality (Di Lillo et al., 2013; Heath et al., 2016a). Significant progress has been made in increasing the level of electrostatic holding force generated, with greater understanding of thin film dielectrics used for EBL devices (Di Lillo et al., 2011) and improved close contact between structurally integrated electrodes through fabrication process enhancements (Heath et al., 2016a). Novel enhancements, namely interlocking electrode elements considered herein, could further improve the performance and application potential of EBL.

Concept

A multitude of parameters influence the level of achievable holding force for electrostatic reversible adhesive devices (Guo et al., 2016). For EBL configurations, with a controlled environment and fabrication process, this list can be reduced to the key parameters of importance for determining the electrostatic force generated between adjacent electrodes. Equation (1) describes the level of electrostatic adhesive holding force expected for EBL devices with an included air region between adjacent electrodes, as well as the known dielectric layer (Mao et al., 2014). The accuracy of this equation and the validity of the configuration with respect to the air layer inclusion, has been previously demonstrated (Heath et al., 2016a).

$$P_N = \frac{\varepsilon_0 \varepsilon_{r1} \varepsilon_{r2}^2 V^2 S}{2(\varepsilon_{r1} d_2 + \varepsilon_{r2} d_1)^2} \quad (1)$$

$$P_\tau = \mu P_N \quad (2)$$

From the parameters shown, several options for increasing the level of electrostatic holding force are apparent, the majority of which are determined by the choice of dielectric medium. The voltage (V) can be maximised, and the electrode separation (the combination of the dielectric thickness (d_1) and the air gap thickness (d_2)) can be minimised. This combination is primarily based on the choice of dielectric, as the maximum operating voltage is dependent on the breakdown voltage of the material, which is dependent on its dielectric strength and thickness. The relative permittivity of the dielectric layer (ε_{r1}) is a material property that should be optimised for a given air gap size. The maximum permissible shear force will be governed by the electrostatic normal force and the friction coefficient, so an increased friction coefficient would also be a desirable material property for the dielectric/electrode interface. The air gap thickness is primarily a function of the fabrication process, and minimising this aids in force enhancement (Heath et al., 2016a). ε_0 is the permittivity of free space (8.854x10-12 Fm^{-1}) and is considered here to be constant. The electrode contact area (S) is a geometric term determined by the chosen EBL design which, for a given fixed geometry, is constant. Within such geometric constraints, adaptations to the electrode surfaces could allow for a greater incorporated electrostatic contact area, potentially increasing the level of holding force generated. The use of non-planar Interlocking Electro-Bonded Laminates (iEBL) is one such adaptation.

In addition to the increased electrode contact area theoretically available when introducing interlocking elements, structural anisotropy is introduced. This can provide useful additional features such as electrode alignment and additional mechanical constraint to motion across the wave peaks (y-direction). Electrode alignment can improve the repeatability of performance, ensuring that the electrode contact area remains constant. The additional mechanical restraint can improve performance in more complex loading environments and provide directionally anisotropic properties, as de-energised iEBL devices would still resist slip in the y-direction, whilst allowing for movement along the x-axis.

Design and Fabrication

For iEBL there exist many possible surface patterns. Any deviation away from the planar configuration will yield an increase in the effective contact area, provided that the surfaces are complementary so as to avoid introducing large air inclusions. Patterning introduction was limited to a single directional axis for two reasons: firstly, complex double curvature significantly increases the manufacturing complexity for the interlocking devices; given the necessity for close contact between the electrodes, processes that could jeopardise the achievement of high tolerance finished parts should be minimised. Secondly, the single directionality of the patterning provides the anisotropy highlighted as a potential benefit of introducing the elements. The cosine wave form in Equation (3) was selected for the iEBL, and held consistent along the x-axis.

$$z = A.\cos\left(\frac{2\pi}{\lambda} y\right) \quad (3)$$

For the overall core width of 30 mm, and a maximum core thickness of 6 mm (geometric restrictions for direct comparison to a previous study (Heath et al., 2016a)), a range of amplitudes and wavelengths were considered. Table 1 shows the resulting change in length from the 30 mm standard width.

Table 1: Theoretical change in effective electrode width

	Amplitude	**Wavelength λ (mm)**				
	A (mm)	**2**	**3**	**5**	**6**	**10**
Change in	**0.5**	13.8	7.0	2.8	2.0	0.7
Width Δw	**1.0**	38.9	21.7	**9.6**	7.0	2.8
(mm)	**2.0**	95.2	57.4	28.5	21.8	9.6

Assuming the electrode lengths are to remain constant, the percentage changes in effective electrode area can be easily calculated. Whilst the shortest wavelength and highest amplitude configuration yields the largest increase in area, some manufacturing and operational constraints exist. Preliminary investigations into sample fabrication revealed issues with bridging and loss of z-direction resolution when using very short wavelengths. Furthermore, in order to ensure that the samples were symmetric about their centre with respect to the *XZ* cross section, only wavelengths with factors of overall width of 30 mm were deemed appropriate. As a result a wavelength of 5 mm and amplitude of 1 mm was chosen for the samples for testing. With a modest increase of 32% in area *S* (from 4200 mm^2 to 5545 mm^2), this was deemed suitable to display an improvement over the planar EBL devices (pEBL), whilst allowing for high quality fabrication. Square and triangular wave forms would introduce sharp vertices to the surface, which could be problematic for manufacture as well as introducing dielectric breakdown initiation locations, thus the cosine wave form was deemed superior. Equations (1) and (2) can be implemented to provide estimates for the electrostatic holding forces generated across the interface for both the pEBL and iEBL configurations. The key parameters are assumed to be a dielectric thickness of 23 μm, a dielectric relative permittivity of 3.3, a friction coefficient of 0.228, a standard planar electrode contact area of 4200 mm^2, and an air gap thicknesses of 3.5 μm, based on the findings of Heath *et al* (Heath et al., 2016a), and assuming the use of Mylar *A* dielectric thin film. The 32% area increase yields a theoretical 32% increase in electrostatic holding force (Table 2). For the thin dielectric used, and considering each infinitesimal width of the electrodes, the electrostatic adhesive force can be assumed to act normal to the local surface. The normal force in Table 2 is the sum of these local normal forces across the electrode width, and not the normal force in the global *z*-direction. The shear holding force is of greatest interest, as this determines the level of shear stress transfer between the upper and lower elements (Heath et al., 2016a), and when subject to a tensile force in the *x*- direction, the resistance to sliding is determined by the product of the surface friction coefficient and the total electrostatic adhesive force.

Table 2: Theoretical increase in electrostatic holding force

		Normal Holding Force (N)		**Shear Holding Force (N)**	
		EBL	**iEBL**	**EBL**	**iEBL**
Voltage	1000	51.4	67.9	11.7	15.5
(V)	2000	205.6	271.4	46.9	61.9

The interlocking EBL devices were fabricated by means of a relatively simple modular process. 6082-T651 aluminium alloy tools of the desired interlocking geometry were first produced using a computer numerical controlled (CNC) machining process. After machining, these parts were bead blasted and then polished using 6, 3 and 1 μm diamond suspensions sequentially. These master components were then used to generate negative silicone moulds (SE2005 Silicone, ACC Silicones Ltd, UK). From these moulds, replica PU interlocking parts were produced (PU-FC, Easy Composites, UK) The electrode elements were added to the host structures using a thin film 18 μm polyimide 25 μm copper laminate (DVL-004-16, GTS Flexible Ltd, UK). The laminate was pre-formed between the metallic interlocking components under 400 kPa (4 bar) pressure, and then bonded to the PU host structures using a laminating epoxy resin (EL2, Easy Composites, UK), curing the resin for 24 hours under vacuum and ambient temperature, completing the fabrication of the samples (Figure 2).

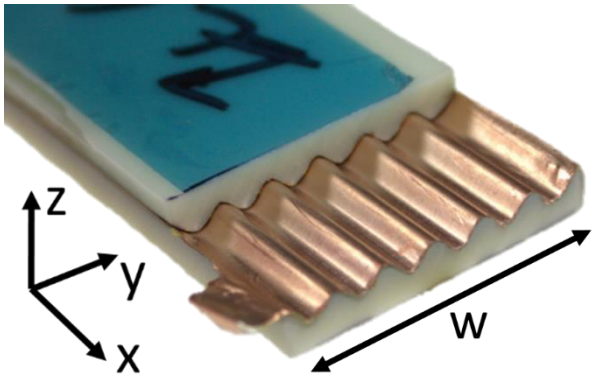

Figure 2: Polyurethane core iEBL device

Experimental

The shear holding strengths of the iEBL and pEBL devices were quantified using a single lap shear test method. Due to the high voltage nature of the devices (up to 2 kV), all testing was carried out within a Poly(methyl methacrylate) (PMMA) safety box. The lower iEBL/pEBL sections were securely mounted within the safety box, and the upper sections connected to an INSTRON 3343 test machine with a 1 kN load cell, using Kevlar thread (6 intertwined strands of Kevlar sewing thread, Easy Composites, UK) via a single pulley. A sled mass of 2 kg was used to preload the samples, and provide a comparative 0 kV shear force value. The applied loading rate was 10 mm/minute, in the global *x*-direction. For the pEBL and iEBL samples, 10 repeat tests were carried out at voltage applications of 0, 1 and 2 kV across the integrated electrodes. These tests were used to assess the peak shear holding force before large scale slippage was observed at the EBL interface. A high voltage DC/DC step up convertor was used to generate the high potential difference for the iEBL/pEBL devices (EMCO F Series, EMCO High voltage Corporation, USA).

Results and Discussion

By observation, the initial PU core iEBL (samples IL_cd) appear to interlock and fit well. Given the requirement for close, micron level contact between the adjacent electrodes for reasonable electrostatic forces to be observed, the electrode surface topography was investigated in greater detail. For a representative section across

the width of the centre of the samples, an optical 3D micro-coordinate system (InfiniteFocus, Alicona Ltd, UK) was used to capture the wave profiles (Figure 3). The close matching of the upper and lower interlocking elements was further confirmed, although localised wave amplitude variations were noted. Despite the close fit, more substantial air gaps exist between the upper and lower iEBL elements. Whilst these defects are likely to be localised and not apparent along the entire length of the samples, a decrease in the electrostatic holding force should be expected.

The shear holding force at the electrostatic interface of EBL devices is key in determining their performance. When the stress at the central interface exceeds a critical value, determined by the electrostatic force and friction properties, slip will occur. The maximum shear force values before slip occurred for each of the investigated voltage values are shown in Figure 4. The values displayed are the corrected value for the increased holding force generated by the activation of the electrostatic devices. The 0 kV average shear force values resulting from the sled mass and frictional forces were 4.48 N for the pEBL sample (IL_P_cd) and 4.46 N for the iEBL sample (IL_cd), suggesting friction coefficients of approximately 0.228. Upon application of a potential difference, the pEBL samples, despite the lower theoretical contact area, display higher average shear holding force before slip occurs. Given the small but visible wave form variations in Figure 3, this decrease in force is not unexpected. Interlocking elements are highly susceptible to small tolerance issues as the two faces must be entirely complementary to preclude larger air inclusions. Creating two complementary planar samples is a less complex task, as high tolerance flat tooling can be used, so air inclusions are based on the low roughness and waviness of the tool used.

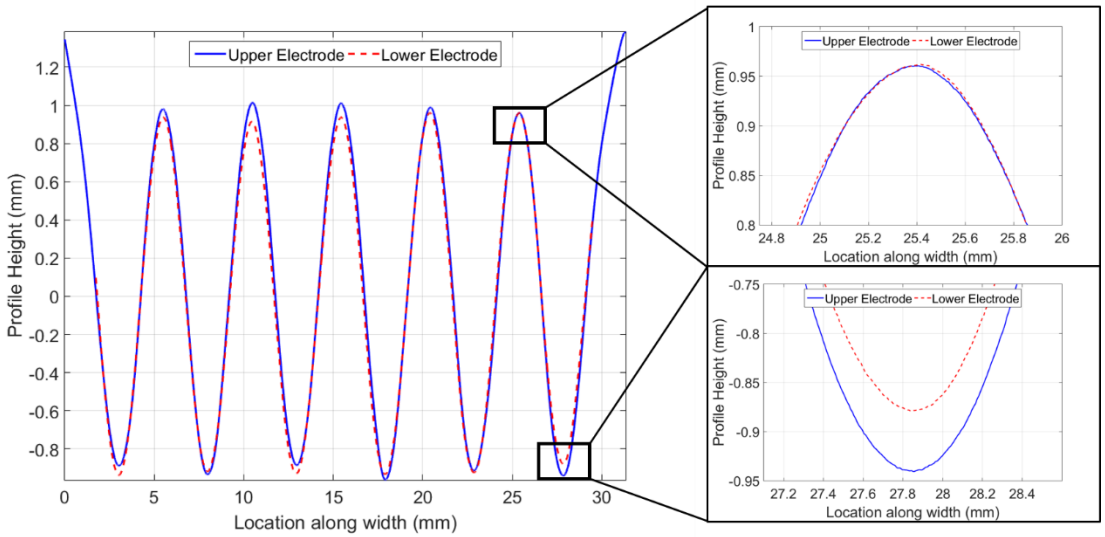

Figure 3: Surface profiles of IEBL with PU core (Sample IL_cd)

Comparing the data in Figure 4 to the expected shear forces from Table 2, all experimental results are lower than the theoretical values. The most likely variable leading to reductions at the 2 kV level is the air gap thickness. Using Equation (1) and maintaining all other key variables constant, an air gap of approximately 4 µm would yield the observed level of shear holding force for the planar sample. Similarly, an air gap of 6.5 µm would yield the level of holding force observed for the iEBL sample. For the pEBL samples, air inclusions are introduced as a result of surface roughness and waviness, and thus topography data has been obtained to verify

this air gap value. For a representative 10 mm by 40 mm area, the average profile height is 3.8 μm which is close to the 4 μm expected level, and the larger deviations from the planar surface are mostly recesses, rather than protuberances. Such recesses introduce local air gaps but not larger scale bridging, which would introduce a large air gap "valley" between two or more pronounced and widely spaced peaks. These findings increase confidence in the validity of the assumptions made for the theoretical calculations.

For the iEBL samples, assessment of the air gap thickness is non-trivial as the air inclusions result from mismatches between the upper and lower surfaces. An average air gap thickness of 6.5 μm does not seem unreasonable, based on the small sample of topography data. The 1 kV data is far below the expected shear holding force levels. This is in line with some existing literature, where the 1 kV values also fell below the expected values, whereas higher voltage results matched the theoretical values more closely (Heath et al., 2016a). The fact this discrepancy was not observed for the tests of EBL devices at lower voltages in the literature perhaps provides a clue to the cause (Di Lillo et al., 2013). The aforementioned tests used thin polyimide copper devices that would have a far increased conformability than the PU mounted devices considered herein, as demonstrated by the low load to deflection behaviour demonstrated in the three-point flexural tests in (Di Lillo et al., 2013). Even at low voltages, flexible EBL devices would allow for a greater degree of 'pull-in' due to the electrostatic force of attraction between the electrodes, potentially further reducing the air gap thickness. For rigid backed EBL, this effect may only be observed when the electrostatic force is sufficient to overcome the additional stiffness of the mounting. A detailed investigation to confirm this is a key requirement for future research. When designing for a specific interface holding force, the potential limitation of rigid backed EBL devices should be considered.

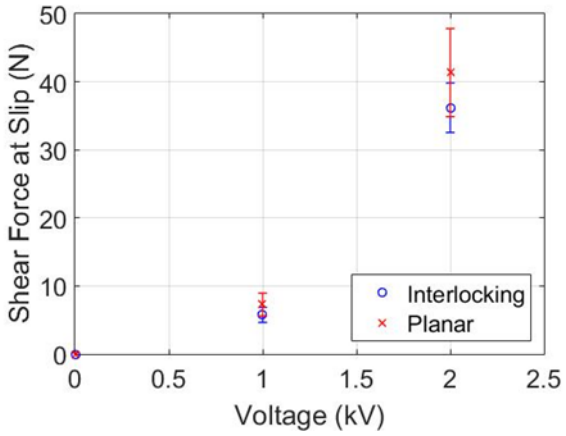

Figure 4: Electrostatic shear force for interlocking vs. planar EBL samples with PU core

The increased air gap thickness resulting from the difficulties of fabricating two perfectly complementary interlocking surfaces, the iEBL devices produced for this study do not demonstrate the anticipated increase in electrostatic holding force arising from increased electrode contact area. The interlocking devices do, however, offer other potential benefits, owing to the non-planar nature of the devices. The interlocking devices ensure that the upper and lower electrodes can be easily aligned, improving repeatability in the observed level of electrostatic holding force, as demonstrated by the lower standard deviation of the tested sample sets. Furthermore, the anisotropic nature of the incorporated core geometry provides additional sliding resistance in

the *y*-direction (across the width of the sample), whilst allowing for sliding in the *x*-direction (along the length of the samples). Using the same arrangement for testing in both the *x*-axis, and *y*-axis directions, Figure 2, the added resistance to sliding provided by the interlocking geometry is evident. In the non-energised 0 kV state, the mean shear force value before sliding in the *y*-direction is over 6 times greater for the iEBL configuration compared to the pEBL, with a mean shear force value of 29.5 ± 1.60 N for the iEBL and 4.46 ± 0.60 N for the pEBL. This anisotropic behaviour thus allows for directionally tailored added functionality.

Conclusions

Non-planar structurally integrated, iEBL devices have been demonstrated, with the devices showing a reversible adhesion level of the same order of magnitude as an equivalent pEBL configuration. At a 2kV applied potential difference, average shear force levels before EBL slip occurs were approximately 41 and 36 N for the pEBL and iEBL respectively (10 and 7 kPa equivalent shear stresses). From surface profile data captured for a representative sample across the width of the iEBL, the interlocking surfaces are for the most part well matched. The close fitting, yielding an assumed average air inclusion layer of only 6.5 μm has been achieved through a relatively non-complex modular fabrication process. Additional enhancement of this process could further reduce the air inclusions resulting from discrepancies between the two interlocking geometries, potentially yielding force levels equivalent or higher than pEBL devices via increased electrode contact area. Despite the slight reduction in electrostatic holding force in this current study (in comparison to pEBL), the added benefit of directional anisotropy that the iEBL devices offer is an example of their significant potential and value for use in reconfigurable or morphing structures. Further enhancement of the fabrication process, along with investigation into the mechanical response of these devices under flexural and torsional loading is ongoing.

Acknowledgements

The Authors wish to thank The James Dyson Foundation for funding this research.

Bibliography

Bergamini A (2009) Electrostatic modification of the bending stiffness of adaptive structures. ETH.

Bergamini A, Christen R, Maag B, et al. (2006) A sandwich beam with electrostatically tunable bending stiffness. *Smart Materials and Structures* 15(3): 678–686.

Bergamini A, Christen R and Motavalli M (2007) Electrostatically tunable bending stiffness in a GFRP–CFRP composite beam. *Smart Materials and Structures* 16(3): 575–582.

Coulomb CA (1785) Premier-[troisième] mémoire sur l'electricité et le magnétisme. Académie Royale des sciences.

Di Lillo L, Carnelli D a, Bergamini a, et al. (2011) Quasi-static electric properties of insulating polymers at a high voltage for electro-bonded laminates. *Smart Materials and Structures* 20(5): 057002.

Di Lillo L, Raither W, Bergamini A, et al. (2013) Tuning the mechanical behaviour of structural elements by electric fields. *Applied Physics Letters* 102(22): 224106.

Guo J, Tailor M, Bamber T, et al. (2016) Investigation of relationship between interfacial electroadhesive force and surface texture. *Journal of Physics D: Applied Physics* 49(3): 35303(9pp).

Heath CJC, Bond IP and Potter KD (2016a) Electrostatic adhesion for added functionality of composite structures. *Smart Materials and Structures*, IOP Publishing 25(2): 11.

Heath CJC, Bond IP and Potter KD (2016b) Variable stiffness sandwich panels using electrostatic interlocking core. In: *SPIE 9799, Active and Passive Smart Structures and Integrated Systems 2016*, Las Vegas, NV, USA, p. 97992A.

Mao J, Qin L and Wang Y (2014) Modeling and simulation of electrostatic attraction force for climbing robots on the conductive wall material. In: *2014 IEEE International Conference on Mechatronics and Automation (ICMA)*, IEEE, pp. 987–992.

Previtali F, Delpero T, Bergamini A, et al. (2015) Multi-functional extremely anisotropic structural element. *Extreme Mechanics Letters*, Elsevier Ltd 3: 82–88.

Raither W, Bergamini A, Gandhi F, et al. (2012) Adaptive bending-twist coupling in laminated composite plates by controllable shear stress transfer. *Composites Part A: Applied Science and Manufacturing*, Elsevier Ltd 43(10): 1709–1716.

Raither W, Heymanns M, Bergamini A, et al. (2013) Morphing wing structure with controllable twist based on adaptive bending–twist coupling. *Smart Materials and Structures* 22(JUNE 2013): 065017.

Raither W, Simoni L De and Lillo L Di (2014) Adaptive-Twist Airfoil Based on Electrostatic Stiffness Variation. In: *AIAA SciTech*.

Tabata O, Konishi S, Cusin P, et al. (2001) Micro fabricated tunable bending stiffness devices. *Sensors and Actuators A: Physical* 89: 119–123.